Study on the capacity fading of pristine and FePO4 coated LiNi1/3Co1/3Mn1/302 by Electrochemical and Magnetical techniques

Study on the capacity fading of pristine and $FePO_4$ coated $LiNi_{1/3}Co_{1/3}Mn_{1/3}O_2$ by Electrochemical and Magnetical techniques

Xizheng Liu,[a,b] De Li,[a] Huiqiao Li,[a] Akira Iyo,[c] Nobuko Hanada,[b] Masayoshi Ishida,[b] and Haoshen Zhou,*[a,b,d]

[a] Energy Technology Research Institute, National Institute of Advanced Industrial Science and Technology (AIST), Umezono 1-1-1, Tsukuba, 305-8568, Japan. Fax: + 81-29-8613489； Tel: + 81-29-8615872； E-mail: hs.zhou@aist.go.jp

[b] Graduate School of System and Information Engineering, University of Tsukuba, Tennoudai 1-1-1, Tsukuba, 305-8573, Japan

[c] Electronics and Photonics Research Institute, National Institute of Advanced Industrial Science and Technology (AIST), Umezono 1-1-1, Tsukuba, 305-8568, Japan

[d] National Laboratory of Solid state Microstructures & Department of Energy Science and Engineering, Nanjing University, Nanjing, 210093, P. R. China

ABSTRACT

Capacity fading mechanism of pristine and $FePO_4$-coated $LiNi_{1/3}Co_{1/3}Mn_{1/3}O_2$ has been studied by electrochemical and magnetic methods. Along with cycles, significant increase of cell polarization and charger transfer resistance (R_{ct}), which mainly cause the capacity fading at the initial charge/discharge cycles, have been observed according to the cyclic voltammetry (CV) and electrochemical impedance spectroscopy (EIS) analysis. In comparison, the existence of $FePO_4$ coating layer can effectively suppress the deterioration of surface polarization and increase of R_{ct} at the interface of electrode/electrolyte. The coated sample suppress the decrease of Li^+ diffusion coefficient with prolonged cycles according to the galvanostatic intermittent titration technique (GITT) tests. It also shows larger Weiss constants (fitting above 130K) and lower blocking temperatures, which indicate the surface coating can suppress the deterioration of Li/Ni disorder upon repeated cycles. This study may give the researchers some light on understanding the capacity fading mechanism of $LiNi_{1/3}Co_{1/3}Mn_{1/3}O_2$ and the effects of surface coating layer, and thus, give help to the future designing of superior coating layers for layered cathode materials in Li-ion batteries.

Keywords: capacity fading, surface coating, Li/Ni disorder, electrochemical, magnetic

Graphical abstract

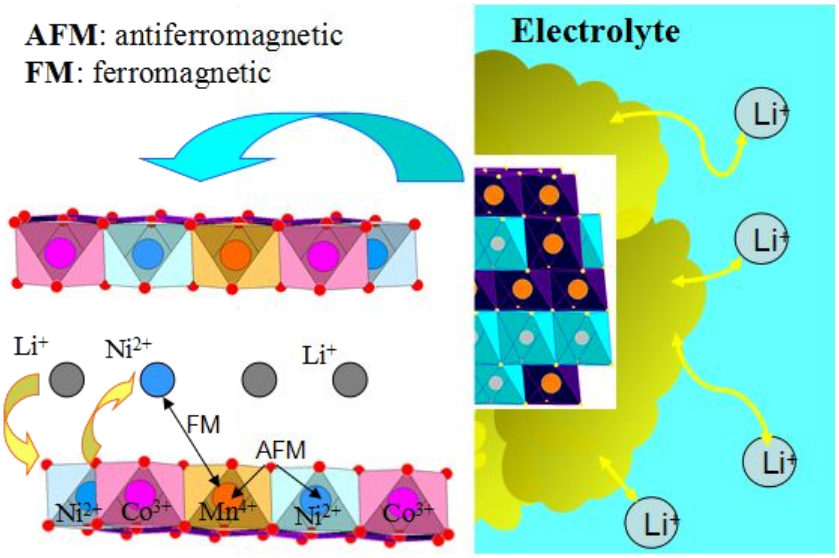

Capacity fading mechanism of pristine and $FePO_4$-coated $LiNi_{1/3}Co_{1/3}Mn_{1/3}O_2$ have been studied by electrochemical and magnetic methods. The $FePO_4$ coating layer takes effect in four aspects: suppress the surface polarization, hinder the increase of R_{ct} at the interface of electrode/electrolyte, impede the decrease of Li^+ diffusion coefficient and the deterioration of Li/Ni disorder with prolonged cycles.

1. Introduction

Lithium ion batteries have attracted intense interest in Hybrid Electric Vehicles (HEV), Electric Vehicles (EV) and smart grid because of its high energy density and long cycle life [1,2]. Electrochemical performances of Li ion batteries critically depend on the electrode composites especially the cathode materials [3]. The continuously increasing requirements of energy, power, cost and safety propel us to explore and develop new cathode materials with better electrochemical performances. $LiNi_{1/3}Co_{1/3}Mn_{1/3}O_2$ has been considered as a very prospective cathode material since it combines the advantages of $LiCoO_2$, $LiNiO_2$ and $LiMnO_2$, and shows much attracting performances such as good cycle life, rate capability and thermal stability [4]. However, it is still faced with several challenges in terms of more widely applications, which typically refer to the capacity fading, increasing of cell resistance and thermal runaway upon long cycles of charge/discharge [5]. Many researchers have endeavored to improve its electrochemical performances by surface coating because the electrochemical behaviors of the electrode are found critically dependent on the surface chemistry [6]. A proper coating material, can not only impede the side-reactions at the interface of electrode and electrolyte, but also provide ion/electron conducting media to facilitate the charge transfer. Various coating materials, such as metal oxides (e.g. Al_2O_3, ZrO_2, CeO_2) [7-9], metal fluorides (e.g. AlF_3, ZrF_2, SrF_2) [5, 10, 11] and many carbon species (Ppy, carbon) [12, 13], have been explored to improve the electrochemical performances of $LiNi_{1/3}Co_{1/3}Mn_{1/3}O_2$. We also investigated the electrochemical performances of $LiNi_{1/3}Co_{1/3}Mn_{1/3}O_2$ with different coating layers such as V_2O_5, PEDOT and $FePO_4$, and found all these coating layers effectively enhanced the electrochemical properties of $LiNi_{1/3}Co_{1/3}Mn_{1/3}O_2$ [14-16]. However, in-depth understanding the role of coating layers during the charge/discharge processes is still inadequate. The mechanism should be further examined in order to design and tailor new coated materials with better electrochemical properties.

GITT method is popularly used to determine the open circuit voltage (OCV) and

lithium ion diffusion coefficient in cathode materials, which can further reflect the lithium-ion dynamics during charge/discharge process. CV measurements at varied scan rates can be used to explore the electrode kinetic behaviors according to the changed separation of cathodic and anodic peaks and currents. EIS can effectively reflect the changes of cell resistance during charge/discharge process and also the changes with increased cycles [17]. Combining all of the above electrochemical analysis techniques, we may get clear images of the Li ion kinetics with increasing charge/discharge cycles and the improvements by surface coating.

Magnetic susceptibility measurements are high sensitive to the changes of local structure of magnetic ions and can elegantly characterize the cations mixing in the layered cathode. A. Mauger et al. associated the cation mixing in layered cathode with magnetic properties, and found that the Ni^{2+} ion in substitution to Li^{+} on the (3b) lattice site, generates a Ni^{2+}(3b)-Mn^{4+}(3a) ferromagnetic interaction. The strengthened ferromagnetic interactions lead to an increase of magnetic ordering temperature [18-21]. The samples with lower cation mixing ratio show better battery performances. Reviewing the relevant literatures, it is noted that most of the published papers are committed to the cation mixing of as-synthesized materials rather than cycled samples. It is lack but highly need to get more informations on the cation mixing evolutions of cycled as well as for coated samples.

In this study, comprehensive investigations on the cycled samples of both pristine and $FePO_4$ coated $LiNi_{1/3}Co_{1/3}Mn_{1/3}O_2$ samples were carried out by combining galvanostatic intermittent titration technique (GITT), cyclic voltammetry (CV), electrochemical impedance spectroscopy (EIS) and magnetic techniques.

2. Experimental

Material preparation and battery assembly

Pristine $LiNi_{1/3}Co_{1/3}Mn_{1/3}O_2$ and 2 wt% $FePO_4$ coated $LiNi_{1/3}Co_{1/3}Mn_{1/3}O_2$ were prepared as our previous work [16]. The pristine $LiNi_{1/3}Co_{1/3}Mn_{1/3}O_2$ was synthesized by co-precipitation method using carbonate as precipitant and sintered at 900 °C for

10 h. The surface $FePO_4$ coating were conducted in aqueous suspension with a coating amount of 2% by weight and heat treated at 400 °C for 5 h. Both of their electrochemical performances were conducted on CR 2032 coin cells consisting of a cathode, a Celgard separator, a lithium metal as the anode, and 1M $LiPF_6$ in EC/DEC (1:1 vol%) as the electrolyte.

Electrochemical performance measurements

The galvanostatic charge/discharge tests were first conducted for desired cycles before taking the GITT, CV and EIS measurements. The tests were performed on Hokuto Denko with a potential range between 2.8-4.5 V. GITT, CV and EIS were conducted on Solartron instrument Model 1287 electrochemical interface. For GITT measurements, the cells were first charged at a constant current density of 20 mA/g for 1 hour and followed by an open circuit stand of the cell for 3 hours between 2.8-4.5 V. CV measurements were conducted in the voltage range of 2.8-4.5 V at different scan rates. EIS were done on Solartron 1255B frequency response analyzer in a frequency range of 0.5 MHz to 0.1 Hz with AC of 5 mV. Data analysis was conducted using the Zview 2.70 software (Scribner Associates Inc., USA).

Magnetic measurements

The magnetic susceptibility measurements were performed with SQUID magnetometer (Quantum Design MPMS XL-7). The temperature dependence of the magnetic susceptibility was recorded in a zero-field cooling (ZFC) mode and the sample was cooled to 4 K under zero-field and then the magnetization was measured upon heating to 300 K after a magnetic field of 1000 Oe was applied. To prepare the sample for test, disassembled the cells after 100 charge/discharge cycles, and then collected the electrode materials from the current collector, washed them by EC/DEC solution and ethanol, respectively, and then dried at 100 °C over night in vacuum. For non-cycled cells, the fresh electrode materials as synthesized were used for measurements.

3. Results and Discussions

The 2 wt%-400 °C $FePO_4$ coated sample was chosen since it showed the best electrochemical performances among the coated samples with various coating amounts and different heat treated temperatures in our previous report [16]. All coated samples showed a well ordered hexagonal α-$NaFeO_2$ structure with R_{3m} space group, as confirmed by the XRD patterns. The $FePO_4$ coating layer was confirmed by SEM, TEM and EDS, it uniformly distributed on the surface of $LiNi_{1/3}Co_{1/3}Mn_{1/3}O_2$. These characterization data have been published in our previous report [16]. The cells were first charge-discharge to the desired cycles at a current of 150 mA/g in a cutoff voltage range of 2.8-4.5 V vs. Li/Li^+. Fig. 1 shows the capacity retentions of both pristine and coated samples with different cycles. An obvious improvement of capacity retention at each certain cycles by surface coating of $FePO_4$ have been confirmed which are consistent with our previous studies [16]. In order to fully understand the performance degradation and the roles of surface coating, further studies on Li ion dynamics especially the evolutions upon cycles are needed. Detailed study of EIS and GITT on different cycled cells combined with the magnetic properties of fresh and 100 cycled samples are presented in the following sections.

Internal resistance is another important factor related to the capacity fading of lithium ion batteries [22]. EIS is a reliable technique to identify the Li ion kinetics and internal resistance in cathode [17, 23]. To gain further understanding on the evolutions of electrochemical properties, 50, 100 and 200 charge/discharge cycled samples were analyzed by EIS at different state of charge, respectively. During the EIS tests, the cells were charged at 20 mA/g for one hour and then relaxed to its open circuit potential (OCP) for 3 h. Then the EIS measurement was performed in the frequency range of 0.5 MHz to 0.1 Hz with an ac signal of 5 mV. This procedure was repeated in the voltage range of 2.8-4.5 V. The Li ion intercalation and de-intercalation during charge and discharge process are normally modeled as a multi-step processes. The Nyquist plots showed two typical semi-circles during the charge processes as shown in Fig.2. It is similar to the previous reports [16]. Generally, the EIS profile can be

expressed by several parts, which in sequence from the high to low frequency are: (I) the ohmic resistance of the electrolyte (R_{sol}), (II) the resistance at the electrode/electrolyte interface and electron pass through the active material, this part can be represented by resistive/capacitive combination because of the electric double layer ($R_f \parallel CPE_f$), (III) the charge transfer resistance and double layer capacitance ($R_{ct} \parallel CPE_{ct}$), (IV) the impedance to the Li ion diffusion in the solid state electrode (Z_w), as introduced by Warburg [7]. In our experiment, some of the Nyquist plots showed no Warburg diffusion due to the frequency limitation. The equivalent circuits which model the elementary reactions were adopted as shown in Fig.2e and 2f. In the equivalent circuit, the capacitance is CPE $\propto A/l$, where A is the geometric surface area and l is the thickness of the surface film. It is well known that the side-reactions with prolonged cycles of pristine $LiNi_{1/3}Co_{1/3}Mn_{1/3}O_2$ lead to the accumulation of by-products on the electrode surface and thus the film thickness l would increase. This can be reflected by the decrease of CPE part in the corresponding equivalent circuits. For the impedance plots of the 200 cycled pristine samples, the low frequency semicircle is absent and only half of the second semi-circuit is observed. So the corresponding circuit elements were excluded from the equivalent circuit (inner the Fig. 2f). All of the quantitative analysis were based on the the equivalent circuit fitting results.

As shown in Fig. 2a, during the charge process, the first semi-circle changed very little even charged the cell to 4.5 V, which indicates the Li ion concentration in the cathode material has relatively small effects on the surface film resistance. By carefully examining the data in Fig. 2b-2d, all of the other cycled cells show similar trends except of the 50 cycled coated samples in Fig. 2c. For coated sample, the coating layer obvious affect the charge transfer route in the electrode surface. The interface resistance of coated sample are also sensitive to the lithium concentrations of the electrode materials. Thus, the Nyquist plots at the high frequence showed significant changes in Fig. 2c. With prolonged cycles, there was complicated side-reactions at the interface of electrolyte/electrode during lithiation/delithiation. It can seriously affected the cathode polarizations and the performance degradations

from the surface deep into the internal of electrode. The charge transfer resistance expressed by the second semi-circle far exceed the first one. Thus, the resistance at the high frequence for long cycled samples became less sentive to the lithium concentration of electrode. For the charge transfer resistance, the surface $FePO_4$ coating layer suppressed the increase of charge-transfer resistance and thus the 50 cycled coated samples showed a comparable surface film resistance and charge transfer resistance. As charging (accompanied by the decreasing of Li ion concentration in the cathode material), the resistance first decreased, then maintained as a constant state and finally increased back to a large value at the end of charge. The observed change trends are similar to the previous reports of $LiNi_{1/3}Co_{1/3}Mn_{1/3}O_2$ and other layered cathode material such as $LiCoO_2$ [17]. The physical processes can be described as: (I) a large resistance appeared at the initial of delithiation, (II) along with the delithiation process, the increased lithium vacancy promote the charge transfer and the resistance decreases, a constant value is obtained at a potential range in consistent with the charge plateau, (III) the resistance increases again at the end of charge due to the increase of interlayer repulsive force at higher delithiation state.

To quantitatively clarify the evolution of R_{ct} with prolonged cycles, the fitting results are shown in Fig.3. With delithiation, the R_{ct} first decreases, then reaches a constant and finally increases again. This trend is similar with the changes of semi-circles in Nyquist plots. These observations confirm that R_{ct} plays an important role in the total resistance of the cells. The R_{ct} reaches a constant at a certain potential which is inconstant with the charge plateau of the corresponding charge process. There is only a small difference of R_{ct} between the 50 cycled cells of pristine and coated samples. With the increase of charge/discharge cycles, rapidly increase of R_{ct} is observed for the pristine samples, and the value of R_{ct} reaches a constant appears at a much higher potential range. For the coated samples, a relatively smaller increase of R_{ct} can be clearly observed. The R_{ct} values for the coated samples after 200 cycles are even smaller than that of 100 cycled pristine samples. These observations can be well correlated with the changes of the charge plateaus at the corresponding cycles as our previous report [16]. The increase of R_{ct} caused kinetics barriers and performance

degradations with prolonged cycles. The improvements of electrochemical performances for $FePO_4$ coated sample can be mainly attributed to the slow increase of R_{ct} values.

Fig. 4a and 4b show the open circuit voltage (OCV) curves after 50, 100 and 200 cycles. The certain cycled cells were first charged at a current of 20 mA/g for 1 h and followed by an open circuit operation for 3 h to allow the cells relaxing to its equilibrium state. In respect to the charge/discharge profiles, similar but more detailed information can be obtained. There is an obvious increase of charge plateaus and decrease of discharge plateaus for the pristine samples at increased cycles. Also the capacity fading can be confirmed by the OCV in Fig. 4a. While, the OCV of coated samples exhibit a limited change of the charge plateau and discharge plateau with the increased cycles. A suppressed capacity and voltage fading by surface coating layer has been obtained. The surface coating layer suppressed the deterioration of electrode polarization. This is coincidence with the charge/discharge profiles analysis.

GITT is established as a powerful technique with high accuracy to determine the Li ion diffusion coefficient D_{Li} to host materials of varying compositions [23-25]. The apparent diffusion coefficient obtained from the GITT is usually used to demonstrate the phase separation and cation ordering in layered cathode materials [24]. To further clarify the kinetics evolution, especially the changes of ionic transport properties with prolonged cycles, the apparent D_{Li} was calculated according to the GITT. The previous study of other researchers on Li ion diffusion coefficients usually involved the battery behaviors in the first several charge/discharge cycles. Few reports have focused on the ionic transport evolution with prolonged cycles. In this section, we not only study the Li ion diffusion coefficient D_{Li} as a function of cycle number, but also compared the change trends between the pristine and coated samples.

The whole GITT process is finished by several titration circles. For each titration circle, the electrode should be first charge/discharge at a constant current density for a limited time period of τ and following a long period of open circuit to reach the equilibrium state. The cells were charged at a constant current flux of 20 mA/g for an interval τ of 1 h, followed by an open circuit stand for 3 h to allow the cell voltage to a

steady state value (E_s). The sequence was repeated in the voltage range of 2.8-4.5 V. The D_{Li} in the cathode materials can be calculated according to the Fick's second law of diffusion. It is found that the single titration of varied cell voltage vs. $t_{1/2}$ (time) showed a straight line behavior. Combined with a series of assumptions and simplifications, the equation can be written as [17, 24]:

$$D_{Li} = \frac{4}{\pi}\left(\frac{m_B V_m}{M_B A}\right)^2 \left(\frac{\Delta E_s}{\Delta E_\tau}\right)^2 \qquad (\tau << L^2 / D_{Li})$$

where m_B is the active mass, V_m is the molar volume of the compound, M_B is the molecular weight, A is the total contact area between the electrode and electrolyte, and L is the thickness of electrode. The ΔE_s and ΔE_τ are the change in the equilibrium state potentials and the total transient change in cell voltage during respective single titration as shown in Fig. 4c. The V_m value deduced from the crystallographic data are 20.1 and 20.3 cm^3/mol for the fresh materials of pristine and coated sample, respectively. We assumed the V_m remains unchanged with the change of Li contents and prolonged cycles. The geometric surface area of the electrode, a round pest with a diameter of 8 mm, is taken as the total contact area A between the electrode and electrolyte. There should be a change of contact area with different cycles because of the deposition of by-products on the electrode surface. However, it is difficult be precisely determined. Therefore, we consider contact area A as a constant in our calculation.

The empirical D_{Li} calculated from the GITT curves (charge process) as a function of cell voltage for different cycled pristine and $FePO_4$ coated samples are plotted in Fig. 4d. In the previous report on the D_{Li} values of pristine $LiNi_{1/3}Co_{1/3}Mn_{1/3}O_2$, a minimum in the plot of D_{Li} vs. voltage was observed, which was regarded as the phase transition or some order-disorder transition during cycling. The minimum of D_{Li} usually appeared at the voltage of 3.7 V [17]. However, there is no minimum D_{Li} in the results of our cycled samples. This might because the first point we got is at a potential of 3.75 V, which is higher than the equilibrium potential of minimum D_{Li}. A D_{Li} value of $1.80*10^{-10}$ cm^2/s at 3.77 V is obtained based on our experiment result, which is in the same order of magnitudes to the previously reported results of

$LiNi_{1/3}Co_{1/3}Mn_{1/3}O_2$ [17].

With the removal of lithium ions, The D_{Li} undergoes a slight increase and then remain stable until the voltage to 4.4 V. The D_{Li} decreases abruptly as further delithiation above 4.4 V, which results from the deep delithiation leading to strengthened attractive force of lithium ions from the oxidized transition metal layer. For long cycled samples, the D_{Li} values of pristine samples decrease more rapidly than those of coated samples at the corresponding lithium concentration of cathode. It is noted that the 50 cycled samples show an exception: the D_{Li} values of pristine is a little bigger than that of the coated samples. The detailed reason is not clear at present. The D_{Li} values of coated samples show a slight decrease compared with those of pristine sample. As we know, the D_{Li} can directly reflect the lithium ion diffusion status inside the active materials. It is probably that a structure rearrangement and local structure changes occurred with the increasing of charge/discharge cycles. Obviously, the surface coating by $FePO_4$ in this study suppressed this tendency. For $LiNi_{1/3}Co_{1/3}Mn_{1/3}O_2$, the most possible structure rearrangement might arise from the disorder of Li and Ni since the diameter of Li^+ (0.76 Å) is very similar to that of Ni^{2+} (0.69 Å). In case of large Li/Ni ion exchange, serious distortion force caused by the ion exchange would lead to irreversible crystal structure transformation, which is definitely detrimental to the cycle life and rate performance. It is necessary to study whether there is a disorder of Li/Ni with the prolonged cycles.

For the layered cathode materials, capacity is highly dependent on the cation order, especially the Li/Ni order. A sample with high ordered structure usually delivers high reversible charge/discharge capacities [26]. Our recent research on $LiNi_{0.42}Mn_{0.42}Co_{0.16}O_2$ showed that sample with a high cation mixing ratio of Li/Ni exhibit an obvious anisotropic stress, smaller inter-slab space of unit cell, and in all negative effects on capacity, cycle and rate performance [27]. However, to our knowledge, it is lack of direct evidence to demonstrate the Li/Ni mixing ratio evolution upon the prolonged charge/discharge cycles. Magnetic technique is an intelligent technique to characterize the cation mixing ratio of layered $Li(NiCoMn)O_2$ and has been recently used to study the cationic order of fresh cathode materials

synthesized at different temperatures [28]. Herein, we did the magnetic studies on both fresh synthesized and 100 cycled $LiNi_{1/3}Co_{1/3}Mn_{1/3}O_2$ samples to see the Li/Ni mixing ratio evolutions with prolonged cycles, and made carefully comparison of cycled pristine and cycled coated samples.

The temperature dependence of the reciprocal magnetic susceptibilities are shown in Fig 5a and b. As described in other's research, at high temperatures, the layered $Li(NiMnCo)O_2$ series compounds are Curie-Weiss paramagnets [28]. As the temperature down, strengthened interlayer and intralayer magnetic interactions lead to a deviation from the Curie-Weiss law. In this research, above 130 K, the linear variations of χ_m^{-1} with T were fitted by Curie-Weiss law: $\chi_m^{-1} = (T - \Theta_p)/C_p$, where Θ_p is the Weiss temperature and C_p is the Curie constant. The values of fitting parameters Θ_p are listed in Tab.1. The negative value of Θ_p reveals an intrinsic dominate antiferromagnetic interaction. Among the possible magnetic interactions, Mn^{4+}-O-Mn^{4+}, Ni^{2+}-O-Ni^{2+} and Mn^{4+}-O-Ni^{2+} via 90° bonding angles, are antiferromagnetic interactions, and the other two are ferromagnetic interactions according to the Kanamori-Goodenough rules [29]. In the studied material, the large negative Θ_p value indicates that the antiferromagnetic interactions held the dominate positions. From the probability point of view, Mn^{4+}-O-Ni^{2+} accounts for half of the intralayer magnetic interactions if the metal ions are uniformly-distributed in $LiNi_{1/3}Co_{1/3}Mn_{1/3}O_2$ compound. The introduce of non-magnetic Co^{3+} would dilute the magnetic interactions, which has been confirmed by previous research [30]. For the fresh synthesized material, there was no significant difference in Θ_p values between the pristine and coated samples. However, after charge/discharge cycles, the Θ_p of the coated samples was -168.74 K, larger than that of cycled pristine sample (-239.68 K). The surface coating suppressed the decrease of Θ_p value upon charge/discharge cycles. As we know, the increase of Li/Ni disorder directly increases the nonmagnetic Li^+ percentage in the transition metal layer, which would reinforce the antiferromagnetic interactions. After charge/discharge cycles, both the Θ_p values of pristine and coated samples decreased, which originated from the increase of Li/Ni disorder. However, the coated sample showed depressed effects on the Li migrations. That is to say, the

surface coating can alleviate the interlayer Li^+ migrations during charge/discharge cycles.

The ZFC susceptibilities of the pristine and coated samples show a cusp at lower temperatures, which is a typical spin-glass transition. In layered $Li(NiCoMn)O_2$, the non-magnetic Co^{3+} and trace of Li^+ in transition metal layers can dilute the magnetic interactions and therefore, the formation of large size magnetic clusters are disturbed and a spin-glass behavior is observed as reported in $LiNi_{0.4}Mn_{0.4}Co_{0.1}O_2$ and $LiNi_{0.45}Mn_{0.45}Co_{0.1}O_2$ previously [28, 30]. In $LiNi_{1/3}Co_{1/3}Mn_{1/3}O_2$, the increase of non-magnetic Co^{3+} further decreases the magnetic clusters and the blocking temperature. As shown in Fig. 6a, the blocking temperatures for pristine and coated $LiNi_{1/3}Co_{1/3}Mn_{1/3}O_2$ are about 7.5K and 7.0 K, respectively. There was no obvious change of the blocking temperature by $FePO_4$ coating since the total amount of $FePO_4$ is only 2 wt% and the magnetic Fe^{3+} ions is less than 0.7 wt% in the final coated material. For the cycled samples shown in Fig. 6b, the cusp appeared at a higher temperature of 9 K for the pristine samples. In contrast, there was no obvious change for the blocking temperature of the coated samples before and after charge/discharge cycles. One of the main reasons for the increase of blocking temperatures of cycled pristine sample can be attributed to the enhanced ferromagnetic interactions. For an ideal atoms arrangement, all of the transition metal cations locate in the transition metal layers and there are only magnetic interactions of Mn^{4+}-O-Ni^{2+}, Mn^{4+}-O-Mn^{4+} and Ni^{2+}-O-Ni^{2+} via 90° bonds inside transition metal layers. As shown in Fig. 6c, the possible migration of Ni^{2+} to the lithium layers can markedly change the M^{n+}-O-M^{n+} bond angles from 90° to 180°. As stated in the last part, the Mn^{4+}-O-Ni^{2+} interactions account for half of the magnetic interactions, which means they govern the overall magnetic behaviors. The magnetic interactions in Mn^{4+}-O-Ni^{2+} are antiferromagnetic via 90° bonds but would transfer to ferromagnetic when the bond angles chang to 180° according to the Kanamori-Goodenough rules [29]. So, the enhanced ferromagnetic interactions of the cycled pristine samples are from the increase of Mn^{4+}-O-Ni^{2+} ferromagnetic interactions via 180° due to the migration of Ni^{2+} to the lithium layer. The unchanged blocking temperature of the coated sample after cycles

demonstrated that there is only few Ni^{2+} migrated to the lithium layer upon charge/discharge cycles, which indicates the Li/Ni disorder upon charge/discharge cycles can be suppressed by surface coating of $FePO_4$ layer.

In general, the performance degradation of layered $LiNi_{1/3}Co_{1/3}Mn_{1/3}O_2$ can be summerized as: the surface polarization appeared at the intial cycles and affect the subsequent cycles. The side-reactions at the electrolyte/electrode interface in the following cycles deteriorate the surface polarization. The charge transfer resistance increased solwly at the initial several cycles, after about 100 cycles, it increased rapidly. The more and more serious of surface polarizaiton lead to the increase of R_{ct}. The increase of R_{ct} can directly lead to a larger energy gap between charge and discharge process [16]. The decrease of Li ion diffusion coefficient and increase of Li/Ni disorder only appeared in high cycle number cells. In the calculated Li ion diffusion coefficients, sharply difference appeared in 100 and 200 cycled samples. This phenomenon demonstrated that the interior deteriorations appeared in high cycled cells. In this paper, we first studied the Li/Ni disorder in cycled layered cathode materials. The cathode materials with high cycle number showed a increase of Li/Ni disorder. It can also result in capacity fading. This is a gradually process from the interface to the internal structure. For the coated sample, the $FePO_4$ coating layer, similar for other coating materials, suppress the side-reactions and hindered the deterioration of internal structure with prolonged cycles.

4. Conclusions

The capacity fading mechanism of $LiNi_{1/3}Co_{1/3}Mn_{1/3}O_2$ cathode and mechanism of performance improvement by surface coating of $FePO_4$, have been investigated. The electrochemical analysis combined with the magnetic studies demonstrated that: with the prolonged charge/discharge cycles, the capacity fading in $LiNi_{1/3}Co_{1/3}Mn_{1/3}O_2$ cathodes were ascribed to four aspects as: (1) more and more serious surface polarizations, (2) gradually increase of charge transfer resistance R_{ct}, (3) decrease of Li ion diffusion coefficient, (4) increase of Li/Ni disorder. The $FePO_4$ coating can depress the above four tendencies. The surface coating layer directly severed as a

protective layer in the interface of electrode/electrolyte. It is usually considered that the coating layer can suppress the interface polarization and help to decrease the charge transfer resistance R_{ct} caused by side-reactions at the interface. In our research, the coated samples also showed enhanced Li ion diffusion coefficients and increase of Li/Ni disorder arrangement with prolonged cycles, however, it is obvious the surface coating layer can not directly take effects on the inner structure. The provided information made us believe that the deterioration of electrode surface lead to Li/Ni disorder with prolonged cycles. It is a gradually processes from surface to inner. This information sets the foundation for further probing internal structural evolutions of the coated materials with prolonged charge/discharge cycles more than 200 cycles, this is under doing in our lab. Results shown in this study can help researchers understand the capacity fading of $LiNi_{1/3}Co_{1/3}Mn_{1/3}O_2$ and effects of surface coating layer, and to further design of proper coating layer for layered cathode materials for Li ion batteries.

ACKNOWLEDGMENT

X. Z. Liu would like to thank Scholarship from MEXT Japan, and Dr. Liang Liu in The University of Tokyo for valuable discussion and suggestions about the magnetic properties.

Present Addresses

* Dr. H. Li is now at College of Materials science and engineering, Huazhong University of Science and Technology

References

1. B. Dunn, H. Kamath, and J. M. Tarascon, Science, 334, (2011) 928-935.

2. J. B. Goodenough, and K. S. Park, J. Am. Chem. Soc., 135, (2013) 1167-1176.

3. J. B. Goodenough, J. Power Source, 174, (2007) 996-1000.

4. T. Ohzuku, and Y. Makimura, Chem. Lett., 30, (2001) 642-643.

5. Y. K. Sun, S. W. Cho, S. W. Lee, C. S. Yoon, and K. Amine, J. Electrochem. Soc., 154 (3),

(2007) A168-A172.

6. K. T. Lee, S. Jeong, and J. Cho, Accounts of Chem. Res., 46(5), (2013) 1161-1170.

7. L. A. Riley, A. V. Atta, A. S. Cavanagh, Y. Yan, S. M. George, P. Liu, A. C. Dillon, S. H. Lee, J. Power Source, 196, (2013) 3317-3324.

8. S. K. Hu, G. H. Cheng, M. Y. Cheng, B. J. Hwang, and R. Santhanam, J. Power Source, 188, (2013) 564-589.

9. M. Wang, F. Wu, Y. F. Su, S. Chen, Sci. Chin. Ser. E, 52, (2009) 2737-2741.

10. S. H. Sun, K. S. Park, and Y. J. Park, J. Power Source, 195, (2009) 6108-6115.

11. K. S. Lee, S. T. Myung, D. W. Kim, and Y. K. Sun, J. Power Source, 196, (2009) 6974-6977.

12. R. B. Shivashankaraiah, H. Manjunatha, K. C. Mahesh, G. S. Suresh, and T. V. Venkatesha, J. Solid State, Electrochem., 16, (2012) 1279-1290.

13. N. N. Sinha, N. Munichandraiah, ACS App. Mater. Inter., 1, (2009) 1241-1249.

14. X. Z. Liu, P, He, H. Q. Li, M. Ishida, and H. S. Zhou, J. Alloys. Com., 552, (2013) 76-82.

15. X. Z. Liu, H. Q. Li, D. Li, M. Ishida, and H. S. Zhou, J. Power Source, 243, (2013) 374-380.

16. X. Z. Liu, H. Q. Li, E. J. Yoo, M. Ishida, and H. S. Zhou, Electrochimica Acta, 83,(2012) 253-258 .

17. K. M. Shaju, G. V. Subba Rao, and B. V. R. Chowdari, J. Electrochem. Soc., 151 (9), (2004) A1324-A1332.

18. X. Y. Zhang, W. J. Jiang, A. Mauger, Q. Lu, F. Gendron, and C. M. Julien, J. Power Source, 195, (2010) 1292-1301.

19. A. M. A. Hashem, A. E. Abdel-Ghany, A. E. Eid, J. Trottier, K. Zaghib, A. Mauger, and C. M. Julien, J. Power Source, 196, (2011) 8632-8637.

20. X. Y. Zhang, A. Mauger, Q. Lu, H. Groult, L. Perrigaud, F. Gendron, and C. M. Julien, Electrochimica Acta, 55, (2010) 6440-6449.

21. Y. Cho, P. Oh, and J. Cho, Nano letter, 13, (2013) 1145-1152.

22. X. F. Bie, F. Du, Y. H. Wang, K. Zhu, H. Ehrenberg, K. Nikolowski, C.Z. Wang, G. Chen, Y. J. Wei, Electrochimica Acta, 97, (2013) 357-363.

23. K. M. Shaju, G. V. S. Rao, B. V. R. Chowdari, J. Mater. Chem., 13, (2003) 106-113,.

24. W. Weppner, and R. A. Huggins, J. Electrochem. Soc., 124 (10), (2003) 1569-1578.

25. J. S. Hong, and J. R. Selman, J. Electrochem. Soc., 147 (9), (2003) 3190-3194.

26. A. A. Ghany, K. Zaghib, F. Gendron, A. Mauger, C. M. Julien, Electrochimica Acta, 52, (2007) 4092-4100.

27. H. J. Yu, Y. M. Qian, M. Otani, D. M. Tang, S. H. Guo, Y. B. Zhu, H. S. Zhou, Energy Emviron. Sci., 7, (2014) 1068-1078.

28. J.Xiao, N.A.Chernova, M.S.Whittingham, Chem.Mater. 20, (2008) 7454-7464.

29. J.B.Goodenough, Magnetism and the Chemical bond, Wiely, New York, 1963.

30. N.A.Chernova, M.Ma, J.Xiao, M.S.Whittingham, J.Breger, C.P.Grey, Chem. Mater. , 19, (2007) 4682-4693.

Table 1. Weiss constants of fresh and cycled samples by fitting the data of Fig.5 with Curie-Weiss equation $\chi_m^{-1}(T)=(T-\theta_p)/C_p$

130K	Pristine (fresh)	Coated (fresh)	Pristine (cycled)	Coated (cycled)
Θ	-120.92	-108.44	-239.68	-168.74
Cp	10.63	11.08	16.23	11.14

Figure Caption

Fig. 1. Capacity retention of both pristine and coated samples with different cycles.

Fig. 2. Nyquist plots at different charge states (black: initial state, red: half charged state, green: fully charged state) on different cycled cells a: pristine after 50 cycles, b: pristine after 200 cycles, c: coated sample after 50 cycles, d: coated sample after 200 cycles, e: the equivalent circuit of all cycled samples, f: the equivalent circuit of pristine after 200 cycles.

Fig. 3. R_{ct} changes at different charged state for both pristine and coated samples with different cycles.

Fig. 4. OCV (open circuit voltage) at different cycled cells for (a) pristine, (b) coated samples; (c) applied current flux and the resulting voltage profile for a single titration; (d) The calculated D_{Li} from the GITT data for the different cycled samples.

Fig. 5 Temperature dependence of inverse magnetic susceptibility of the fresh (a) and cycled samples (b). The Curie-Weiss ($\chi_m^{-1}(T)=(T-\theta_p)/C_p$) fit was applied to these data above the temperature of 130K to calculate the Weiss constants.

Fig. 6 Magnetic susceptibility fresh (a) and cycled (b), schematic of magnetic interactions between Mn^{4+} and Ni^{2+} in different layers, (c) model of Li/Ni disorder.

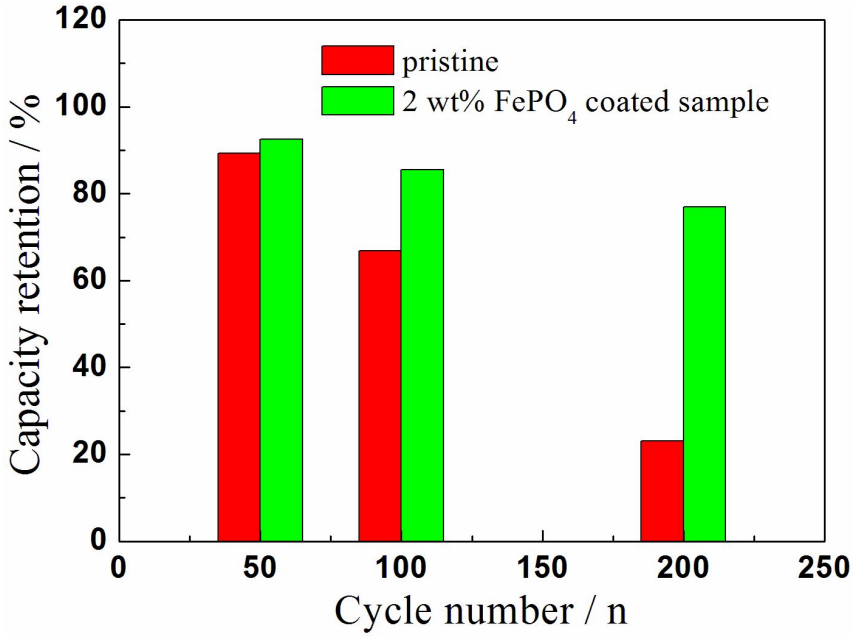
120
100
80
60
40
20
0
0
50
100
150
200
250
Capacity retention / %
Cycle number / n
pristine
2 wt% FePO4 coated sample

Figure 1.

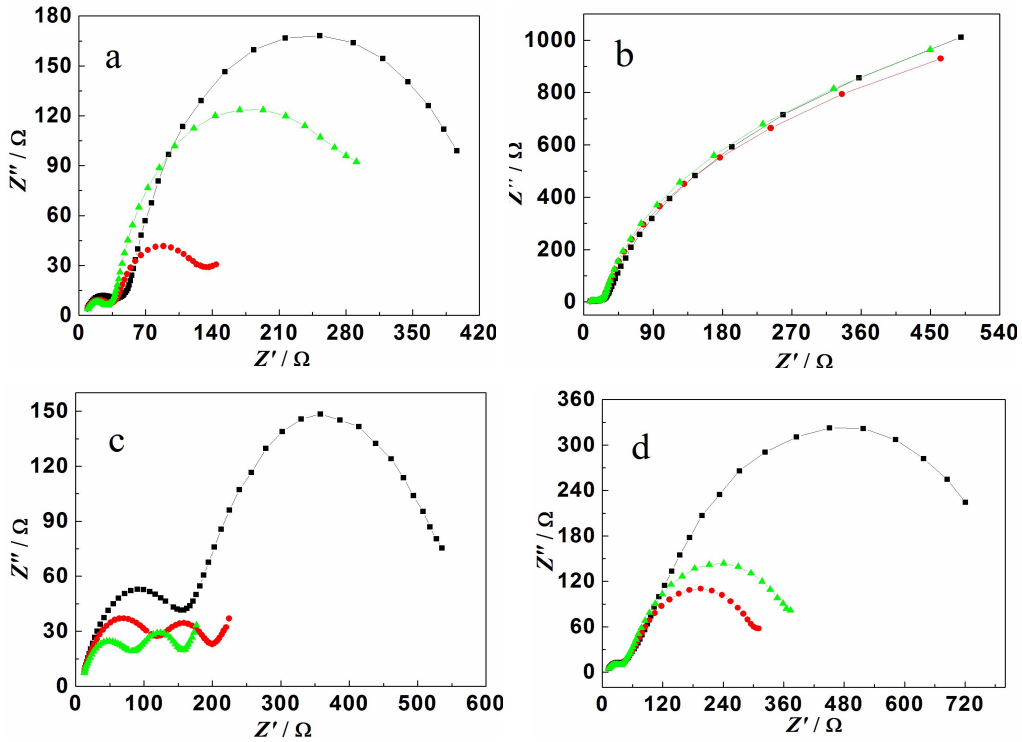

e

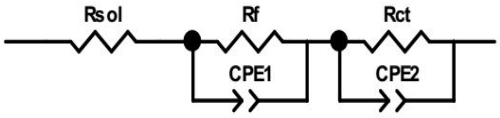

f

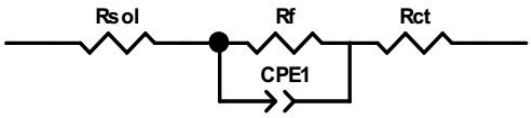

Figure 2.

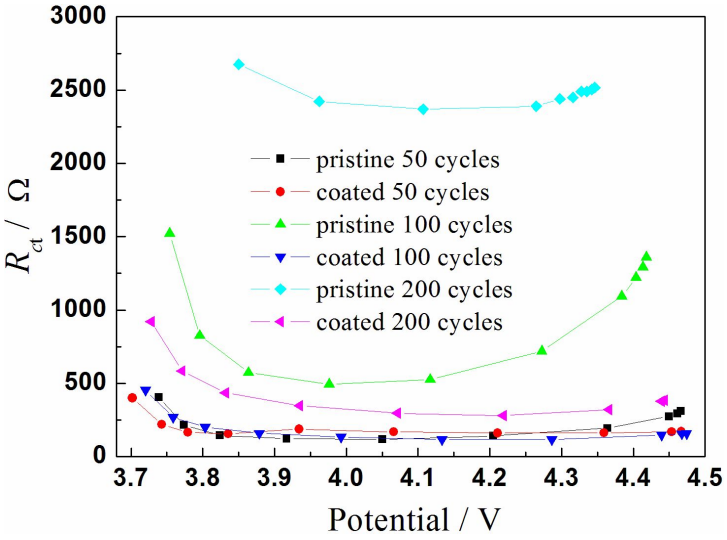
3000
2500
2000
1500
1000
500
0
R_{ct} / Ω
3.7
3.8
3.9
4.0
4.1
4.2
4.3
4.4
4.5
Potential / V
pristine 50 cycles
coated 50 cycles
pristine 100 cycles
coated 100 cycles
pristine 200 cycles
coated 200 cycles

Figure 3.

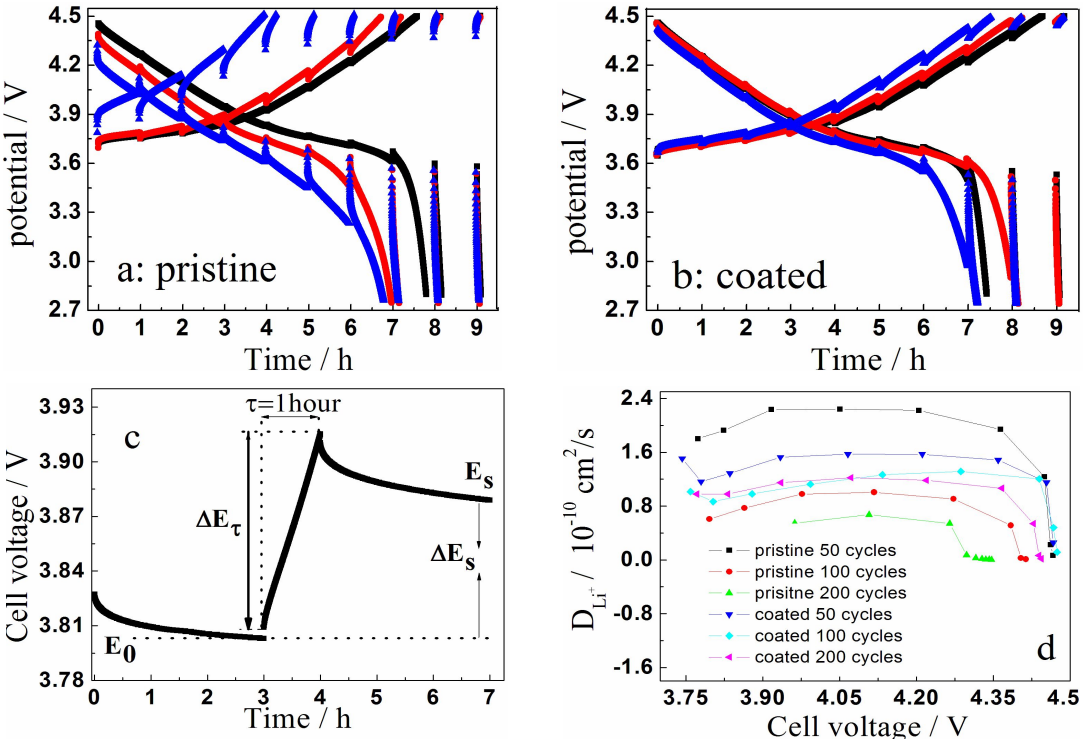
potential / V
a: pristine
Time / h
b: coated
c
τ=1hour
ΔE_τ
E_s
ΔE_s
E_0
Cell voltage / V
D_{Li^+} / 10^{-10} cm^2/s
pristine 50 cycles
pristine 100 cycles
prisitne 200 cycles
coated 50 cycles
coated 100 cycles
coated 200 cycles
d
Cell voltage / V

Figure 4.

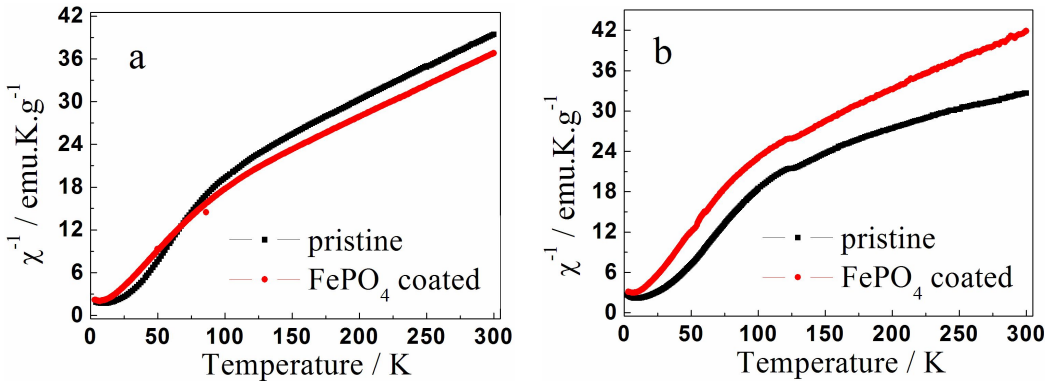
a
b
pristine
FePO4 coated
χ-1 / emu.K.g-1
Temperature / K
0
6
12
18
24
30
36
42
0
50
100
150
200
250
300

Figure 5.

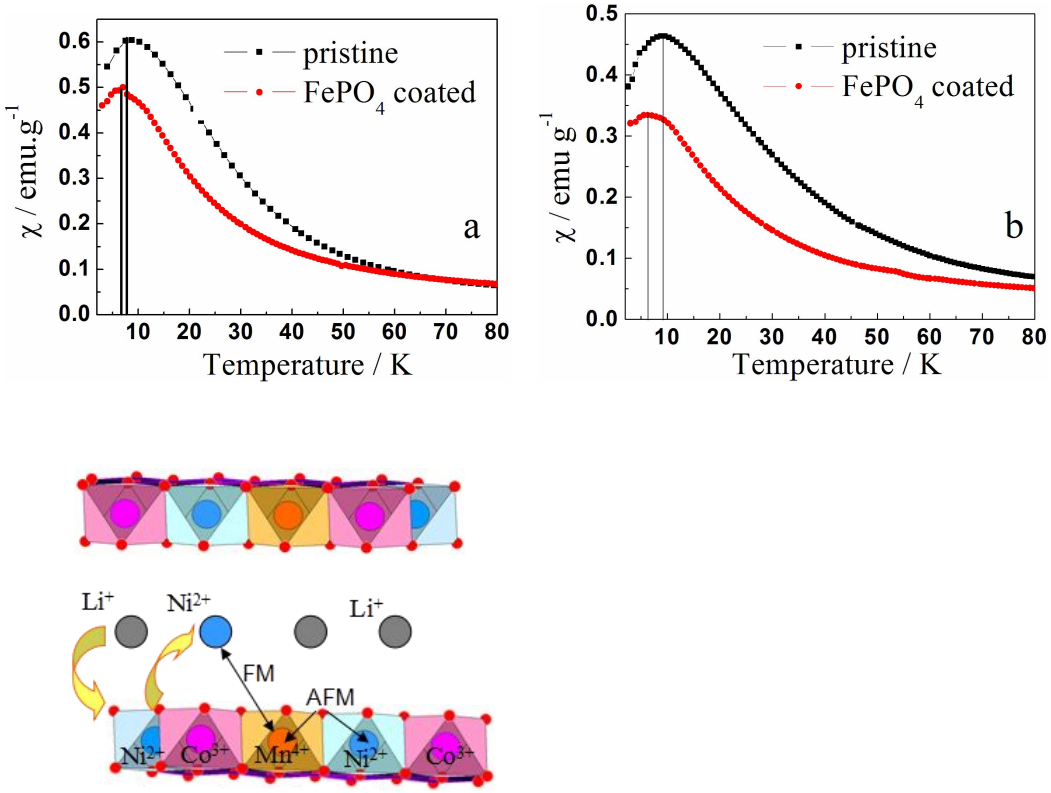
pristine
FePO4 coated
χ / emu.g-1
Temperature / K
a
b
Li+
Ni2+
FM
AFM
Ni2+
Co3+
Mn4+
Ni2+
Co3+

Figure 6.